Rapid Determination of Enantiomeric Excess of α-Chiral Cyclohexanones Using Circular Dichroism Spectroscopy
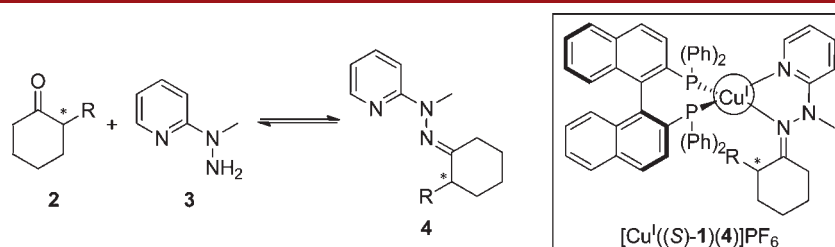
Diana Leung and Eric V. Anslyn*

Department of Chemistry and Biochemistry, The University of Texas at Austin, Austin, Texas 78712, United States

anslyn@austin.utexas.edu

ABSTRACT

Ketone handedness was discriminated using circular dichroism (CD) spectroscopy by monitoring the metal-to-ligand charge transfer (MLCT) bands of complexes between $[Cu^I((S)-1)(CH_3CN)_2]PF_6$ and derivatized α-chiral cyclohexanones (4). This method was able to quantify the enantiomeric excess of unknown samples using a calibration curve, giving an absolute error of ±7%. The analysis was fast, allowing potential application of this assay in high-throughput screening (HTS).

Asymmetric synthesis is well-recognized as a cost-effective method for the production of enantiomerically pure products.[1] Combinatorial methods combined with high-throughput screening (HTS) have become a tool for finding appropriate catalysts/auxiliaries for asymmetric synthesis due to the allowance for a large number of candidates to be rapidly examined. However, the determination of the enantiomeric excess (*ee*) of reaction products is a limiting factor in catalyst discovery. Chromatographic techniques are commonly used to determine *ee* due to their high accuracy, but the intrinsically serial analysis restricts their ultimate use in HTS.[2]

Optical signaling techniques are well adapted for HTS because they use instruments such as circular dichroism (CD) spectrophotometers, fluorimeters, and UV−vis spectrophotometers, which require less time for analysis compared to chromatographic techniques. Typically, a single measurement can be conducted in under a minute, allowing for rapid analysis of samples for HTS of asymmetric catalysts/auxiliaries. Due to the advantage of speed, numerous techniques using optical signaling approaches have been investigated for the determination of *ee*.[3−7] These optical signaling techniques have the advantage that they can be transitioned to a microwell plate format, allowing

(1) (a) Tsukamoto, M.; Kagan, H. B. *Adv. Synth. Catal.* **2002**, *344*, 453. (b) Charbonneau, V.; Ogilvie, W. W. *Mini-Rev. Org. Chem.* **2005**, *2*, 313.

(2) Traverse, J. F.; Snapper, M. L. *Drug Discovery Today* **2002**, *7*, 1002.

(3) Molecular Sensors: (a) Nieto, S.; Dragna, J. M.; Anslyn, E. V. *Chem.—Eur. J.* **2010**, *16*, 227. (b) Nieto, S.; Lynch, V. M.; Anslyn, E. V.; Kim, H.; Chin, J. *Org. Lett.* **2008**, *10*, 5167. (c) Nieto, S.; Lynch, V. M.; Anslyn, E. V.; Kim, H.; Chin, J. *J. Am. Chem. Soc.* **2008**, *130*, 9232. (d) Leung, D.; Anslyn, E. V. *J. Am. Chem. Soc.* **2008**, *130*, 12328. (e) Leung, D.; Folmer-Andersen, J. F.; Lynch, V. M.; Anslyn, E. V. *J. Am. Chem. Soc.* **2008**, *130*, 12318. (f) Shabbir, S. H.; Regan, C. J.; Anslyn, E. V. *Proc. Natl. Acad. Sci. U.S.A., Early Edition* **2009**, 1. (g) Zhu, L.; Shabbir, S. H.; Anslyn, E. V. *Chem.—Eur. J.* **2006**, *13*, 99. (h) Liu, S.; Pestano, J. P. C.; Wolf, C. *J. Org. Chem.* **2008**, *73*, 4267. (i) Richard, G. I.; Marwani, H. M.; Jiang, S.; Fakayode, S. O.; Lowry, M.; Strongin, R. M.; Warner, I. M. *Appl. Spectrosc.* **2008**, *62*, 476. (j) Wolf, C.; Liu, S.; Reinhardt, B. C. *Chem. Commun.* **2006**, 4242. (k) Corradini, R.; Paganuzzi, C.; Marchelli, R.; Pagliari, S.; Dossena, A.; Duchateau, A. *J. Inclusion Phenom. Macrocyclic Chem.* **2007**, *57*, 625. (l) Corradini, R.; Paganuzzi, C.; Marchelli, R.; Pagliari, S.; Sforza, S.; Dossena, A.; Galaverna, G.; Duchateau, A. *J. Mater. Chem.* **2005**, *15*, 2741.

(4) IR thermography: (a) Reetz, M. T.; Becker, M. H.; Kuhling, K. M.; Holzwarth, A. *Angew. Chem., Int. Ed.* **1998**, *37*, 2647. (b) Reetz, M. T.; Becker, M. H.; Liebl, M.; Furstner, A. *Angew. Chem., Int. Ed.* **2000**, *39*, 1236. (c) Reetz, M. T.; Hermes, M.; Becker, M. H. *Appl. Microbiol. Biotechnol.* **2001**, *55*, 531. (d) Millot, N.; Borman, P.; Anson, M. S.; Campbell, I. B.; Macdonald, S. J. F.; Mahmoudian, M. *Org. Process Res. Dev.* **2002**, *6*, 463.

for an even more rapid means of analysis compared to single-cuvette analyses.

Here we demonstrate the use of CD spectroscopy to determine *ee* values of α-chiral cyclohexanones. An analyte binding event that would induce CD signals in wavelengths longer than 320 nm was sought because the analytes themselves, most organic functional groups, and organic solvents are CD silent in this region. This would potentially allow the technique to be used on crude reaction mixtures without purification, making the analysis step even more rapid. For these purposes, the chiral metal complex used in this study was the 2,2′-bis(diphenylphosphino)-1,1′-binaphthyl (BINAP) copper(I) complex ([Cu^I(**1**)(CH$_3$CN)$_2$]PF$_6$). Previous studies have shown that the CD active MLCT bands (Figure 1) are modulated by complexation of chiral analytes, allowing for enantioselective discrimination.[3a,c]
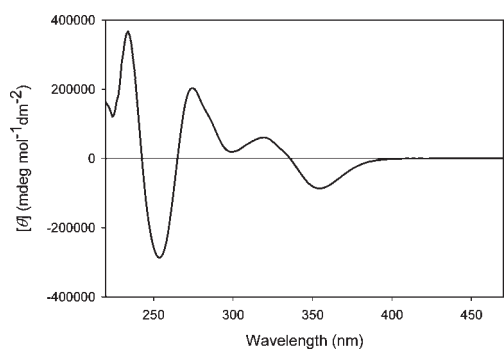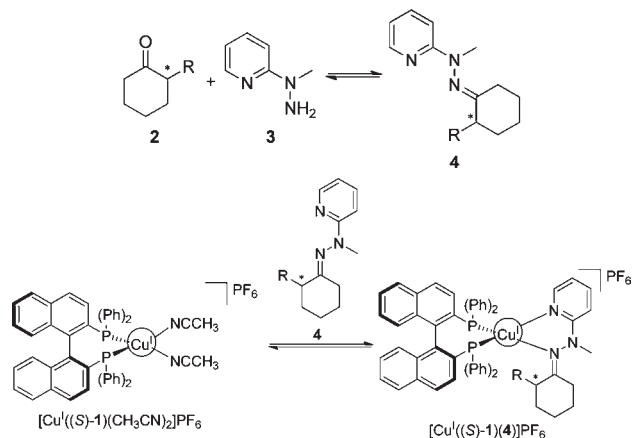

Figure 1. CD spectra of [Cu^I((*S*)-**1**)(CH$_3$CN)$_2$]PF$_6$ (400 μM) in CH$_3$CN.

Scheme 1. Derivatization of α-Chiral Cyclohexanones (**2**) with 1-Methyl-1-(2-pyridyl) Hydrazine (**3**) To Produce a Bidentate Analyte (**4**), Followed by Complexation to [Cu^I((*S*)-**1**)(CH$_3$CN)$_2$]PF$_6$ To Produce [Cu^I((*S*)-**1**)(**4**)]PF$_6$

The analytes targeted in this study, α-chiral cyclohexanones (**2**), presented a challenge due to their limited

number of functional handles to complex to the Cu(I) metal center. To create ligands, they were derivatized with 1-methyl-1-(2-pyridyl) hydrazine (**3**) to produce bidentate hydrazones **4** (Scheme 1).

We postulated that enantioselective discrimination of **4** by the chiral BINAP complex could arise via different twist angles that the two enantiomers of **4** impart on the naphthyl rings in **1**. As shown in Figure 2, (*S*)-**4** is predicted to impart a smaller change in the twist of the two naphthyl moieties of [Cu^I((*S*)-**1**)(CH$_3$CN)$_2$]PF$_6$. This is due to the avoidance of steric interactions between the R-group and the phosphine ligand. On the other hand, binding of the enantiomer (*R*)-**4** induces a steric clash between the substituent in (*R*)-**4** and the phosphine ligand, potentially inducing a larger twist to prevent such interactions. This postulate is illustrated by the Newman projection of the two diastereomeric complexes, [Cu^I((*S*)-**1**)((*R*)-**4**)]PF$_6$ and [Cu^I((*S*)-**1**)((*S*)-**4**)]PF$_6$ in Figure 2. As discussed below, such twists are reflected in the CD spectra, where the predicted disfavored diastereomeric complexes have a larger change in their CD signals from the initial MLCT band of [Cu^I((*S*)-**1**)(CH$_3$CN)$_2$]PF$_6$. By monitoring this change, chiral analytes can be enantioselectively discriminated.
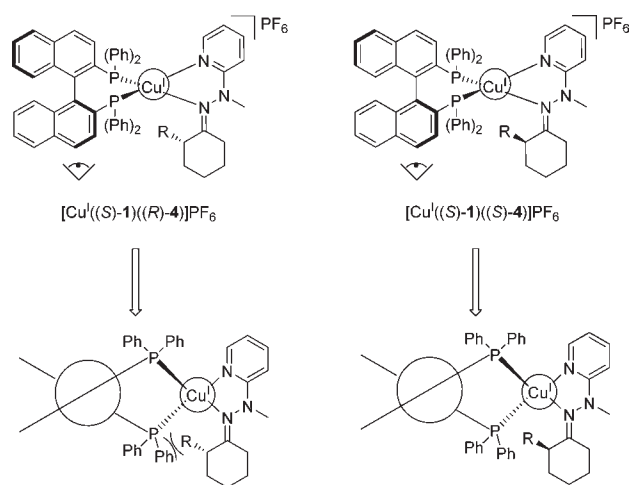
Figure 2. Steric interactions allowing for enantioselective discrimination of hydrazone **4** with [Cu^I((*S*)-**1**)(CH$_3$CN)$_2$]PF$_6$.

Because there are only a few enantiomerically pure commercially available α-chiral cyclohexanones, some of our analytes needed to be synthesized. Oxidation with pyridinium chlorochromate (PCC) of commercially

(5) Liquid Crystals: (a) Eelkema, R.; van Delden, R. A.; Feringa, B. L. *Angew. Chem., Int. Ed.* **2004**, *43*, 5013. (b) van Delden, R. A.; Feringa, B. L. *Chem. Commun. (Cambridge, U.K.)* **2002**, 174. (c) Van Delden, R. A.; Feringa, B. L. *Angew. Chem., Int. Ed.* **2001**, *40*, 3198. (d) Walba, D. M.; Eshdat, L.; Korblova, E.; Shao, R.; Clark, N. A. *Angew. Chem., Int. Ed.* **2007**, *46*, 1473.

(6) Molecular Imprinted Polymers: Shimizu, K. D.; Snapper, M. L.; Hoveyda, A. H. *Chem.—Eur. J.* **1998**, *4*, 1885.

(7) Enzymes/Antibodies: (a) Abato, P.; Seto, C. T. *J. Am. Chem. Soc.* **2001**, *123*, 9206. (b) Onaran, M. B.; Seto, C. T. *J. Org. Chem.* **2003**, *68*, 8136. (c) Dey, S.; Karukurichi, K. R.; Shen, W.; Berkowitz, D. B. *J. Am. Chem. Soc.* **2005**, *127*, 8610.

available enantiomerically pure alcohols 2-phenylcyclo-hexanol and 2-(2-phenylpropan-2-yl)cyclohexanol produced enantiomerically pure ketones 2-phenylcyclohex-anone and 2-(2-phenylpropan-2-yl)cyclohexanone, respectively. Using a polarimeter, the optical rotations of each ketone's enantiomer pair were confirmed to be equal and opposite. In addition, the molar optical rotation of 2-phenylcyclohexanone had been previously reported in the literature, and our sample was found to be in agreement.[8]

Derivatization of enantiomerically pure (R)- and (S)-2-phenylcyclohexanone with hydrazine **3** produced hydra-zone **5**, while 2-(2-phenylpropan-2-yl)cyclohexanone did not react with hydrazine **3**. This was most likely due to the bulky substituent at the α-position of 2-(2-phenylpropan-2-yl)-cyclohexanone. Fortunately, derivatization of (R,S)- and (S,R)-menthone with hydrazine **3** produced hydrazones **6** as a second analyte.

5   **6**
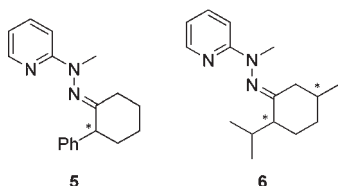
Condensation of hydrazine **3** with α-chiral ketone **2** creates two isomers (E)- and (Z)-**4** (Figure 3). Through HR-MS analysis of the hydrazones **5** and **6**, one peak was found for each compound, correlating to their $[M + H]^+$. However, in the ^{13}C NMR studies, it was observed that duplicate peaks were present, which did not correlate to the starting material. One set of peaks had a significantly smaller intensity and chemical shifts close to the major peaks. In addition, the ^1H NMR showed extra smaller sets of peaks, whose chemical shifts were also similar to the major peaks. This lead us to conclude that both (E)- and (Z)-isomers have been formed. Although two isomers were present, no purification was performed, since the relative ratio of isomers was consistent each time the reaction was conducted (see Supporting Information). Due to the steric clash between the methyl group and the R-substituent on the α-position of (Z)-**4**, the dominant product from the condensation was postulated to be (E)-**4**.
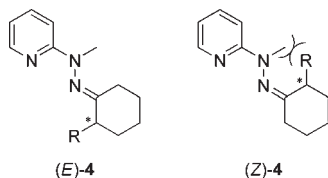

(E)-**4**   (Z)-**4**

Figure 3. (E)- and (Z)-hydrazone produced upon derivatization of α-chiral ketone (**2**) with hydrazine **3**.

One might argue that a technique requiring derivatiza-tion of the analyte for the determination of ee is not amenable for HTS of asymmetric catalysts/auxiliaries,

but this step is a single addition to the time of analysis for all samples. The derivatization step can be carried out in parallel for all the samples requiring analysis, especially since HTS of catalysts/auxiliaries often uses microreactors. Hence, this synthetic step (5−26 h) can potentially be incorporated into the asymmetric reaction scheme.

Upon obtaining derivatized enantiomerically pure hy-drazones, **5** and **6**, titrations with $[Cu^I((S)$-**1**$)(CH_3CN)_2]$-PF_6 were conducted to determine the assay's ability to discriminate the enantiomers. There was no CD signal in the visible region from either enantiomers of **6**, nor from the enantiomers of **6** with the Cu(I) source, $[Cu^I(CH_3CN)_4]PF_6$ (see Supporting Information). A large CD signal was observed for $[Cu^I((S)$-**1**$)(CH_3CN)_2]PF_6$, $[Cu^I((S)$-**1**$)((R,S)$-**6**$)]PF_6$, and $[Cu^I((S)$-**1**$)((S,R)$-**6**$)]PF_6$ (Figure 4). The MLCT bands are different for each enantiomer of **6**, allowing for enantioselective discrimination.

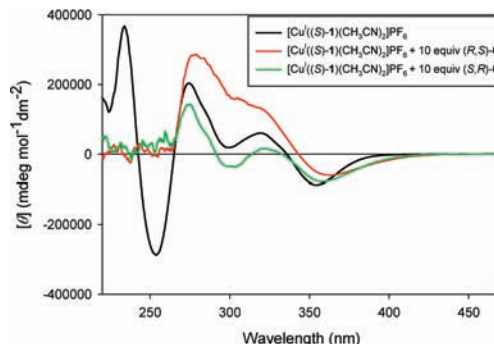**Figure 4.** CD spectra of $[Cu^I((S)$-**1**$)(CH_3CN)_2]PF_6$ (401 μM) in CH_3CN (black), $[Cu^I((S)$-**1**$)(CH_3CN)_2]PF_6$ (401 μM) mixed with (R,S)-**6** (4 mM) (red), and $[Cu^I((S)$-**1**$)(CH_3CN)_2]PF_6$ (401 μM) mixed with (S,R)-**6** (4 mM) (green).

The molar ellipticity of the MLCT band at 350 nm ($λ_{max}$ of the MLCT band) was monitored during a titration, and the enantiomers of **6** were discriminated as shown in Figure 5a. After being able to enantioselectively discriminate **6** with $[Cu^I((S)$-**1**$)(CH_3CN)_2]PF_6$, the scope of this study was extended to target **5**. As shown in Figure 5b, hydrazone **5** was also successfully enantioselectively discriminated, although to a lesser degree.

The enantiomer that induced the largest signal change was (R,S)-**6**, which correlates to the hypothesis that the enantiomer with an (R)-α-stereocenter would lead to more steric interactions with the BINAP moiety, forcing a larger twist of the naphthyl rings, and a larger change in the MLCT band. This was also true of analyte **5**, as shown by the larger change in the MLCT band for (R)-**5** compared to (S)-**5**.

To demonstrate the assay's ability to determine en-antiomeric excess values of unknown samples, a cali-bration curve was generated by monitoring the molar ellipticity at 350 nm with different ee solutions of **5**

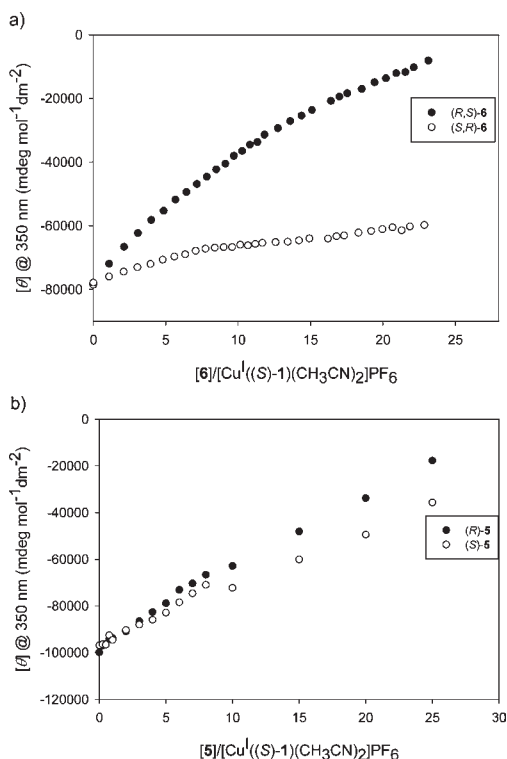(8) Johnson, C. R.; Zeller, J. R. *Tetrahedron* **1984**, *40*, 1225.

Figure 5. CD isotherm at 350 nm with the addition of (a) (*R*,*S*)- or (*S*,*R*)-**6** (15.4 and 19.1 mM, respectively) into a solution of [Cu^I((*S*)-**1**)(CH$_3$CN)$_2$]PF$_6$ (398 μM) in CH$_3$CN. (b) (*R*)- or (*S*)-**5** (18.1 and 22.2 mM, respectively) into a solution of [Cu^I((*S*)-**1**)-(CH$_3$CN)$_2$]PF$_6$ (400 μM) in CH$_3$CN.

100%) with small signal change, the rest of the calibration curve (−100% to 50%) shows significant curvature. The use of the enantiomeric host [Cu^I((*R*)-**1**)(CH$_3$CN)$_2$]PF$_6$ will produce a mirror image calibration curve whose region of maximum signal change closely corresponds to that of minimum signal change from the [Cu^I((*S*)-**1**)(CH$_3$CN)$_2$]-PF$_6$ host shown. Thanks to this property, using both receptors separately should make it possible to differentiate between even closely separated *ee* samples across the whole *ee* range.
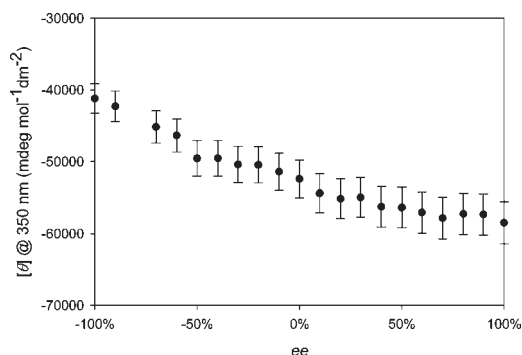

Figure 6. Molar ellipticity at 350 nm with ±5% error bars as a function of *ee* performed with the addition of **5** (10 mM) into a solution of [Cu^I((*S*)-**1**)(CH$_3$CN)$_2$]PF$_6$ (400 μM) in CH$_3$CN.

titrated into enantiomerically pure [Cu^I((*S*)-**1**)(CH$_3$CN)$_2$]PF$_6$ (Figure 6). The *ee* calibration curve was subjected to linear and second-degree polynomial regression, and the best-fit curve was used to determine the *ee* of five independently prepared unknown samples. The calibration curve had considerable scatter, and yet, as now described, the determination of *ee* values for unknown samples was quite accurate. Errors were calculated for each sample by taking the absolute difference between the actual *ee* and the experimentally determined *ee*. The average absolute error for determining the *ee* of **5** for the five unknown samples was ±6.6%.

Though the calibration curve using the [Cu^I((*S*)-**1**)-(CH$_3$CN)$_2$]PF$_6$ host (Figure 6) has a region (50%−

In summary, using commercially available [Cu^I((*S*)-**1**)-(CH$_3$CN)$_2$]PF$_6$, α-chiral cyclohexanones were enantioselectively discriminated using circular dichroism spectroscopy. The speed at which CD operates is advantageous for high-throughput screening of asymmetric catalysts/auxiliaries. We have demonstrated this system's ability to discriminate enantiomers of derivatized cyclohexanones and determine the *ee* of unknown samples with approximately ±7% absolute error.

Supporting Information Available. Experimental procedures, ^{1}H and ^{13}C NMR data, spectral data, and *ee* determinations. This information is available free of charge via the Internet at http://pubs.acs.org.